Error Probability Trade-off in Quantum Hypothesis Testing via the Nussbaum–Szkoła Mapping

Error Probability Trade-off in Quantum Hypothesis Testing via the Nussbaum-Szkoła Mapping

Gonzalo Vazquez-Vilar† and Jorge Lizarribar-Carrillo
Universidad Carlos III de Madrid, Spain
Email: gvazquez@ieee.org

***Abstract*—The error probability trade-off of quantum hypothesis testing is related to that of a certain surrogate classical hypothesis test via the Nussbaum-Szkoła mapping. This connection was used in the information-theoretic literature to establish the asymptotic error exponent of Bayesian quantum hypothesis testing and asymmetric quantum hypothesis testing (Hoeffding bound). In this work, we analyze the non-asymptotic gap between the error probability of a quantum test and the corresponding classical test via the Nussbaum-Szkoła mapping.**

I. Introduction

We study the problem of discriminating between two quantum states. Specifically, let us consider the density operators[1] ρ and σ, acting on some finite dimensional complex Hilbert space $\mathcal{H}$ with dimension d, and define the hypotheses

$$\mathrm{H}_0 : \ \rho, \qquad \mathrm{H}_1 : \ \sigma. \tag{1}$$

In this binary setting we distinguish between two error types:

- The type-I error occurs when accepting H_1 when the true state is the null hypothesis $\mathrm{H}_0 \colon \rho$.
- The type-II error is the error of accepting H_0 when the true system state is $\mathrm{H}_1 \colon \sigma$.

A binary test is defined by a positive self-adjoint operator Π acting on $\mathcal{H}$ such that $0 \preceq \Pi \preceq \mathbb{1}$, where $\mathbb{1}$ denotes the identity matrix and the notation $A \preceq B$ means that $B - A$ is positive semidefinite. For a test Π associated to H_1, let $\bar{\Pi} \triangleq \mathbb{1} - \Pi$. The type-I and type-II error probabilities are, respectively,

$$\alpha(\Pi) = \mathrm{Tr}[\Pi\rho], \tag{2}$$

$$\beta(\Pi) = \mathrm{Tr}[\bar{\Pi}\sigma] = 1 - \mathrm{Tr}[\Pi\sigma]. \tag{3}$$

The two error probabilities cannot be made arbitrarily small at the same time. The best achievable trade-off between these probabilities is given by the Pareto optimal boundary

$$\alpha^\star_\beta(\rho, \sigma) = \inf_{\Pi: \beta(\Pi) \le \beta} \alpha(\Pi). \tag{4}$$

When the alternatives are n-fold tensor products, i.e., $\rho \equiv \rho^{\otimes n}$ and $\sigma \equiv \sigma^{\otimes n}$, previous results established the asymptotic exponential behavior of the type-I and type-II error probabilities as $n \to \infty$. Several of these asymptotic results were obtained using a mapping, first proposed by Nussbaum and Szkoła in [1], that relates the quantum testing problem to a classical one with the same asymptotic exponential behavior.

In this work, we study the Nussbaum-Szkoła mapping in the non-asymptotic setting of fixed n. We analyze its properties and highlight the distinctions between quantum and classical testing problems through specific examples.

The organization of the remainder of the article is as follows. In Sec. II, we summarize some relevant asymptotic results and introduce the Nussbaum-Szkoła mapping. In Sec. III we present bounds on the error probability trade-off and show their tightness under certain conditions. Finally, Sec. IV closes this work with several numerical examples and some final remarks.

II. Preliminaries

For a test between the alternatives $\mathrm{H}_0 \colon \rho^{\otimes n}$ and $\mathrm{H}_1 : \sigma^{\otimes n}$, we consider three significant asymptotic regimes as $n \to \infty$:

1) In a Bayesian setting with prior probabilities $\Pr[\mathrm{H}_0] = \eta$ and $\Pr[\mathrm{H}_1] = 1 - \eta$, the optimal average error probability is:

$$\epsilon^\star_\eta\big(\rho^{\otimes n}, \sigma^{\otimes n}\big) = \inf_{0 \preceq \Pi \preceq \mathbb{1}} \big\{\eta\alpha(\Pi) + (1-\eta)\beta(\Pi)\big\}. \tag{5}$$

The asymptotic exponential analysis of this probability leads to the quantum Chernoff bound [1], [2] (see also [3, Sec. 3]):

$$\limsup_{n\to\infty} -\frac{1}{n} \log \epsilon^\star_\eta\big(\rho^{\otimes n}, \sigma^{\otimes n}\big) = \sup_{0 \le s \le 1} \Big\{ -\log \mathrm{Tr}\big[\rho^{1-s}\sigma^s\big]\Big\}. \tag{6}$$

2) In a non-Bayesian setting with a fixed type-II error β, the optimal type-I error is given by $\alpha^\star_\beta(\rho^{\otimes n}, \sigma^{\otimes n})$. Its exponential behavior corresponds to the quantum Stein's Lemma [4], [5]:

$$\limsup_{n\to\infty} -\frac{1}{n} \log \alpha^\star_\beta(\rho^{\otimes n}, \sigma^{\otimes n}) = \mathrm{Tr}\big[\sigma\big(\log\sigma - \log\rho\big)\big]. \tag{7}$$

3) Enforcing an exponential decrease in the type-II error as $\beta_n = e^{-nr}$, the Hoeffding bound asserts that [6], [7]:

$$\limsup_{n\to\infty} -\frac{1}{n} \log \alpha^\star_{\beta_n}(\rho^{\otimes n}, \sigma^{\otimes n}) = \sup_{0 \le s \le 1} \left\{ \frac{1}{s-1} \log \mathrm{Tr}\big[\rho^{1-s}\sigma^s\big] + \frac{s}{s-1} r \right\}. \tag{8}$$

Two important information metrics appear in these results: the quantum extension of the Renyi and the Kullback-Leibler divergences between density operators σ and ρ are defined as

$$D_s(\sigma\|\rho) \triangleq \frac{1}{s-1} \log \mathrm{Tr}\big[\rho^{1-s}\sigma^s\big], \tag{9}$$

$$D_{\mathrm{KL}}(\sigma\|\rho) \triangleq \mathrm{Tr}\big[\sigma\big(\log\sigma - \log\rho\big)\big] = \lim_{s\to 1} D_s(\sigma\|\rho). \tag{10}$$

†G. Vazquez-Vilar is also with the Gregorio Marañón Health Research Institute, Madrid, Spain. This work has been funded in part by the Spanish Ministry for Science and Innovation under Grant PID2020116683GB-C21 / AEI / 10.13039/501100011033.

[1]Density operators are self-adjoint, positive semidefinite and have unit trace.

A. The Nussbaum-Szkoła Mapping

We consider the eigen-decomposition of the quantum states:

$$\rho = \sum_{i=1}^{d} \lambda_i \left|x_i\right\rangle \left\langle x_i\right|, \qquad \sigma = \sum_{j=1}^{d} \mu_j \left|y_j\right\rangle \left\langle y_j\right|. \tag{11}$$

The Nussbaum-Szkoła mapping transforms the states ρ and σ in two classical distributions P and Q which are defined as

$$p_{i,j} = \lambda_i \left|\langle x_i \,|\, y_j\rangle\right|^2, \qquad q_{i,j} = \mu_j \left|\langle x_i \,|\, y_j\rangle\right|^2, \tag{12}$$

for $i, j = 1, \ldots, d$. For this mapping, it follows that [3, Prop. 1]

$$\mathrm{Tr}\big[\rho^{1-s}\sigma^s\big] = \sum_{i,j} p_{i,j}^{1-s} q_{i,j}^{s}. \tag{13}$$

Then, the quantum Renyi and Kullback-Leibler divergences (9)-(10) coincide with their classical counterparts:

$$D_s(\sigma\|\rho) = D_s(Q\|P) \triangleq \frac{1}{s-1}\log\sum_{i,j} p_{i,j}^{1-s} q_{i,j}^{s}, \tag{14}$$

$$D_{\mathrm{KL}}(\sigma\|\rho) = D_{\mathrm{KL}}(Q\|P) \triangleq \sum_{i,j} q_{i,j}\big(\log q_{i,j} - \log p_{i,j}\big). \tag{15}$$

It follows that the exponential behavior of the quantum test $\rho^{\otimes n}$ v. $\sigma^{\otimes n}$ and that of the classical test $P^{\otimes n}$ v. $Q^{\otimes n}$ coincide in the three asymptotic regimes considered above. Given this (maybe) surprising property, one may wonder about how these tests compare in the non-asymptotic setting of fixed n.

III. Non-asymptotic Analysis

Let $\alpha^{\star}_{\beta}(P,Q)$ denote the error probability trade-off of a classical hypothesis test between the distributions P and Q.[2]

Theorem 1: For a binary quantum hypothesis test between states ρ and σ, and for the classical distributions P and Q defined via the Nussbaum-Szkoła mapping (12), it follows that

$$\alpha^{\star}_{\beta}(\rho,\sigma) \geq \frac{1}{2}\alpha^{\star}_{2\beta}(P,Q), \tag{16}$$

for any $\beta \in \big[0, \frac{1}{2}\big]$, and trivially $\alpha^{\star}_{\beta}(\rho,\sigma) \geq 0$ for $\beta \in \big(\frac{1}{2}, 1\big]$.

Proof: This result corresponds to [3, Prop. 2], which is stated for the average error probability in a Bayesian setting. Using the same technique, in Sec. III-A we give a direct proof for the bound on the error probability trade-off $\alpha^{\star}_{\beta}(\cdot)$. ■

The inequality (16) implies that the optimal error probability trade-off of the quantum test ρ v. σ is lower bounded by that of the classical test when both the type-I and type-II error probabilities α and β are multiplied by $1/2$. Obviously, this lower bound also applies to curve of the classical test P v. Q.

Analogously, applying a change of variable $\alpha' \leftrightarrow 2\alpha$, $\beta' \leftrightarrow 2\beta$ in (16), we conclude that the optimal error probability trade-off of both the quantum test and that of the classical test is upper bounded by the quantum curve when both the type-I and type-II error probabilities are multiplied by 2.

In Sec. IV, we illustrate the accuracy of these bounds through numerical experiments. Prior to that, we prove the main result, and we show that this non-asymptotic bound is indeed tight for specific symmetric discrimination problems.

[2] The function $\alpha^{\star}_{\beta}(P,Q)$ coincides with (4) when ρ and σ are diagonal operators with the distributions P and Q in their respective diagonals.

A. Proof of Theorem 1

The proof of Theorem 1 is based on the following variational formulation of the optimal trade-off $\alpha^{\star}_{\beta}(\cdot)$. For fixed $t \geq 0$, let $\Pi_t \triangleq \big\{t\sigma - \rho \geq 0\big\}$ be the projector onto the non-negative eigenspace of $t\sigma - \rho$, and $\bar{\Pi}_t \triangleq \mathbb{1} - \Pi_t$. Then, [8, Lemma 2]

$$\alpha^{\star}_{\beta}(\rho,\sigma) = \sup_{t\geq 0}\Big\{\mathrm{Tr}\big(\rho\Pi_t\big) + t\big(\mathrm{Tr}\big(\sigma\bar{\Pi}_t\big) - \beta\big)\Big\}. \tag{17}$$

Using the eigendecompositions of ρ and σ from (11), together with the cyclic property of the trace, then (17) yields

$$\alpha^{\star}_{\beta}(\rho,\sigma) = \sup_{t\geq 0}\Big\{\sum\nolimits_{i} \lambda_i \left\langle x_i\right| \Pi_t \left|x_i\right\rangle + t\sum\nolimits_{j} \mu_j \left\langle y_j\right| \bar{\Pi}_t \left|y_j\right\rangle - t\beta\Big\}. \tag{18}$$

For the projectors Π_t and $\bar{\Pi}_t$, it holds that $\Pi_t = \Pi_t\mathbb{1}\Pi_t$ and $\bar{\Pi}_t = \bar{\Pi}_t\mathbb{1}\bar{\Pi}_t$. Moreover, the identity operator can be decomposed as $\mathbb{1} = \sum_i \left|x_i\right\rangle\left\langle x_i\right| = \sum_j \left|y_j\right\rangle\left\langle y_j\right|$. Therefore, after some algebra, we shall rewrite (18) as:

$$\alpha^{\star}_{\beta}(\rho,\sigma) = \sup_{t\geq 0}\Big\{\sum\nolimits_{i,j} \lambda_i \big|\left\langle x_i\right| \Pi_t \left|y_j\right\rangle\big|^2 + t\sum\nolimits_{i,j} \mu_j \big|\left\langle x_i\right| \bar{\Pi}_t \left|y_j\right\rangle\big|^2 - t\beta\Big\}. \tag{19}$$

We group the two sums and we focus on the (i,j)-th addend

$$\begin{aligned}
&\lambda_i \big|\left\langle x_i\right| \Pi_t \left|y_j\right\rangle\big|^2 + t\mu_j \big|\left\langle x_i\right| \bar{\Pi}_t \left|y_j\right\rangle\big|^2 \\
&\quad\geq \min(\lambda_i, t\mu_j)\Big(\big|\left\langle x_i\right| \Pi_t \left|y_j\right\rangle\big|^2 + \big|\left\langle x_i\right| \bar{\Pi}_t \left|y_j\right\rangle\big|^2\Big) && (20)\\
&\quad\geq \frac{1}{2}\min(\lambda_i, t\mu_j)\left(\big|\left\langle x_i\right| \Pi_t \left|y_j\right\rangle\big| + \big|\left\langle x_i\right| \bar{\Pi}_t \left|y_j\right\rangle\big|\right)^2 && (21)\\
&\quad\geq \frac{1}{2}\min(\lambda_i, t\mu_j)\left|\left\langle x_i\right| \Pi_t \left|y_j\right\rangle + \left\langle x_i\right| \bar{\Pi}_t \left|y_j\right\rangle\right|^2, && (22)
\end{aligned}$$

where in (20) we used that both λ_i and $t\mu_j$ are lower bounded by $\min(\lambda_i, t\mu_j)$; in (21) we defined the vector $u = [\left\langle x_i\right| \Pi_t \left|y_j\right\rangle \;\; \left\langle x_i\right| \bar{\Pi}_t \left|y_j\right\rangle]^T$ featuring $k = 2$ dimensions, and applied the norm inequality $\|u\|_2 \geq \frac{1}{\sqrt{k}}\|u\|_1$, $u \in \mathbb{C}^k$; and in the last step (22) we used that $|u_1| + |u_2| \geq |u_1 + u_2|$.

Applying the inequality chain (20)-(22) to the addends in (19) for each (i,j), and recalling that $\Pi_t + \bar{\Pi}_t = \mathbb{1}$, hence $\left\langle x_i\right| \Pi_t \left|y_j\right\rangle + \left\langle x_i\right| \bar{\Pi}_t \left|y_j\right\rangle = \left\langle x_i | y_j\right\rangle$, we obtain

$$\alpha^{\star}_{\beta}(\rho,\sigma) \geq \sup_{t\geq 0}\bigg\{\frac{1}{2}\sum\nolimits_{i,j}\min(\lambda_i, t\mu_j)\big|\left\langle x_i | y_j\right\rangle\big|^2 - t\beta\bigg\}. \tag{23}$$

Using the definitions of P and Q in (12), we note that

$$\min(\lambda_i, t\mu_j)\big|\left\langle x_i | y_j\right\rangle\big|^2 = p_{i,j}1_{[\lambda_i \leq t\mu_j]} + tq_{i,j}1_{[\lambda_i > t\mu_j]}, \tag{24}$$

where $1_{\mathcal{E}}$ denotes the indicator function for the event $\mathcal{E}$.

Particularizing the variational formulation (17) for ρ, σ being diagonal operators with P, Q in their diagonal, it yields:

$$\alpha^{\star}_{\beta}(P,Q) = \sup_{t\geq 0}\Big\{\sum\nolimits_{i,j} p_{i,j}1_{[p_{i,j} \leq tq_{i,j}]} + t\Big(\sum\nolimits_{i,j} q_{i,j}1_{[p_{i,j} > tq_{i,j}]} - \beta\Big)\Big\}, \tag{25}$$

Therefore, noting that for the distributions P and Q in (12), $[p_{i,j} \leq tq_{i,j}] \Leftrightarrow [\lambda_i \leq t\mu_j]$, moving the factor $\frac{1}{2}$ out of the maximization in (23) (using that $\beta = \frac{1}{2}2\beta$), we obtain the desired lower bound (16) from (23)-(24) using (25).

B. Pure-state discrimination and symmetric error probability

We now consider a testing problem between two pure states,

$$\mathrm{H}_0:\ \rho = |x_1\rangle\langle x_1|, \tag{26}$$
$$\mathrm{H}_1:\ \sigma = |y_1\rangle\langle y_1|, \tag{27}$$

where $|x_1\rangle$ and $|y_1\rangle$ are assumed to satisfy $0 < |\langle x_1|y_1\rangle|^2 < 1$. We apply one step of the Gram-Schmidt process and define:

$$|x_2\rangle = \frac{|y_1\rangle - |x_1\rangle\langle x_1\,|\,y_1\rangle}{\||y_1\rangle - |x_1\rangle\langle x_1\,|\,y_1\rangle\|}, \tag{28}$$
$$|y_2\rangle = \frac{|x_1\rangle - |y_1\rangle\langle y_1\,|\,x_1\rangle}{\||x_1\rangle - |y_1\rangle\langle y_1\,|\,x_1\rangle\|}. \tag{29}$$

Both the orthonormal basis $\{|x_1\rangle, |x_2\rangle\}$ and $\{|y_1\rangle, |y_2\rangle\}$ span the same 2-dimensional subspace encompassing $|x_1\rangle$ and $|y_1\rangle$. If the dimension of the underlying Hilbert space is $d > 2$, the remaining eigenvectors $|x_3\rangle, \ldots, |x_d\rangle$ and $|y_3\rangle, \ldots, |y_d\rangle$ are orthogonal to both $|x_1\rangle$ and $|y_1\rangle$, and they become irrelevant in the sequel. In Fig. 1(a), we illustrate a 2-dimensional example of these bases for certain $\rho = |x_1\rangle\langle x_1|$ and $\sigma = |y_1\rangle\langle y_1|$.

1) Classical test: For the eigendecompositions of ρ and σ defined above, the Nussbaum-Szkoła mapping from (12) yields

$$p_{i,j} = \begin{cases} |\langle x_1|y_j\rangle|^2, & i=1,\ j=1,2,\\ 0, & \text{otherwise,}\end{cases} \tag{30}$$
$$q_{i,j} = \begin{cases} |\langle x_i|y_1\rangle|^2, & i=1,2,\ j=1,\\ 0, & \text{otherwise.}\end{cases} \tag{31}$$

The distributions P and Q exhibit non-overlapping supports, except in the singular case $(i,j)=(1,1)$, under which

$$p_{1,1} = q_{1,1} = |\langle x_1|y_1\rangle|^2 = \mathrm{Tr}[\rho\sigma] \triangleq a. \tag{32}$$

Here we defined $a = |\langle x_1|y_1\rangle|^2$ for future convenience.

The optimal classical test for this problem decides the correct hypothesis with no error, except when $(i,j)=(1,1)$. For this observation, in the symmetric setting, the optimal test may select between H_0 and H_1 at random with equal probability, hence incurring an error with probabilities

$$\alpha^{\mathrm{c}} = \tfrac{1}{2}p_{1,1} = \tfrac{1}{2}a, \qquad \beta^{\mathrm{c}} = \tfrac{1}{2}q_{1,1} = \tfrac{1}{2}a. \tag{33}$$

2) Quantum test: A binary test $\Pi = |x_2\rangle\langle x_2|$ does not yield a symmetric error probability in the measurement process. Neither it does the test $\Pi = |y_1\rangle\langle y_1|$. Instead, we construct a symmetric measurement $\Pi = |v_y\rangle\langle v_y|$, $\bar{\Pi} \triangleq \mathbb{1} - \Pi$, with

$$|v_x\rangle \triangleq \frac{|x_1\rangle + |y_2\rangle}{\||x_1\rangle + |y_2\rangle\|}, \tag{34}$$
$$|v_y\rangle \triangleq \frac{|y_1\rangle + |x_2\rangle}{\||y_1\rangle + |x_2\rangle\|}. \tag{35}$$

The vector $|v_x\rangle$ (resp. $|v_y\rangle$) corresponds to the normalized vector which is exactly at the midpoint between $|x_1\rangle$ and $|y_2\rangle$ (resp. between $|y_1\rangle$ and $|x_2\rangle$). It can be verified that these vectors are orthogonal, $\langle v_x|v_y\rangle = 0$, and that they define an orthonormal basis of the subspace spanned by $\{|x_1\rangle, |y_1\rangle\}$. This basis is depicted in Fig. 1(b) for illustration purposes.

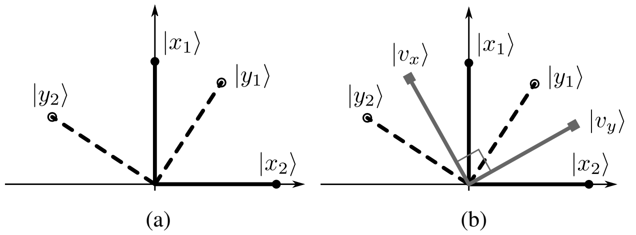

Fig. 1: Hypothesis test between pure states $|x_1\rangle$ and $|y_1\rangle$, with $0 < |\langle x_1|y_1\rangle|^2 \le \frac{1}{2}$. (a) Basis $\{|x_1\rangle, |x_2\rangle\}$ (solid) and $\{|y_1\rangle, |y_2\rangle\}$ (dashed). (b) Orthogonal symmetric measurement $\{|v_x\rangle, |v_y\rangle\}$ (solid gray) for testing between $|x_1\rangle$ and $|y_1\rangle$.

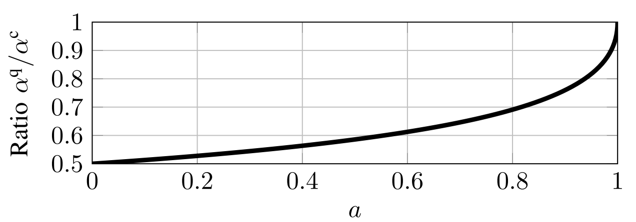

Fig. 2: Ratio between $\alpha^{\mathrm{q}} = \beta^{\mathrm{q}}$ and $\alpha^{\mathrm{c}} = \beta^{\mathrm{c}}$ for a hypothesis test between pure states $|x_1\rangle$ and $|y_1\rangle$, versus $a = |\langle x_1|y_1\rangle|^2$.

We now derive the error probabilities for this quantum test:

$$\alpha^{\mathrm{q}} = \mathrm{Tr}\big[\rho\,|v_y\rangle\langle v_y|\big], \qquad \beta^{\mathrm{q}} = \mathrm{Tr}\big[\sigma\,|v_x\rangle\langle v_x|\big]. \tag{36}$$

We first note that

$$\mathrm{Tr}\big[\rho\,|v_y\rangle\langle v_y|\big] = \mathrm{Tr}\big[\,|x_1\rangle\langle x_1|\cdot|v_y\rangle\langle v_y|\big] = |\langle x_1|v_y\rangle|^2, \tag{37}$$

and, using (35), we write

$$|\langle x_1|v_y\rangle|^2 = \frac{\big|\langle x_1|y_1\rangle + \langle x_1|x_2\rangle\big|^2}{\||y_1\rangle + |x_2\rangle\|^2} = \frac{a}{2\big(1+\sqrt{1-a}\big)}. \tag{38}$$

In the last step we used that $\langle x_1|x_2\rangle = 0$ and $\big|\langle x_1|y_1\rangle\big|^2 = a$; and then we used (28) to obtain, after some straightforward algebra, that $\||y_1\rangle + |x_2\rangle\|^2 = 2\big(1+\sqrt{1-a}\big)$.

According to (36)-(38) and given the symmetry of the problem, the type-I and type-II error probabilities are thus

$$\alpha^{\mathrm{q}} = \beta^{\mathrm{q}} = \frac{a}{2\big(1+\sqrt{1-a}\big)}, \tag{39}$$

which depend only on $a = |\langle x_1|y_1\rangle|^2$.

Figure 2 shows the ratio between $\alpha^{\mathrm{q}} = \beta^{\mathrm{q}}$ and the classical error probability $\alpha^{\mathrm{c}} = \beta^{\mathrm{c}} = \frac{1}{2}a$ as a function of a. We observe that, as a tends to 0 (i.e., states $|x_1\rangle$ and $|y_1\rangle$ approaching orthogonality), this ratio tends to $\frac{1}{2}$. Indeed, using the Taylor expansion of $f(a) \triangleq \frac{a}{2(1+\sqrt{1-a})}$ around $a = 0$, it yields

$$\alpha^{\mathrm{q}} = \beta^{\mathrm{q}} = \tfrac{1}{4}a + o(a), \tag{40}$$

where $o(a)$ satisfies $\lim_{a\to 0}\frac{o(a)}{a} = 0$ (little-o notation).

Therefore, up to a vanishing term $o(a)$, the quantum error probabilities $\alpha^{\mathrm{q}} = \beta^{\mathrm{q}}$ coincide with the lower bound from Theorem 1, given by $\frac{1}{2}\alpha^{\mathrm{c}} = \frac{1}{2}\beta^{\mathrm{c}}$. We conclude that the bound in Theorem 1 is tight in certain scenarios, even when $n = 1$.

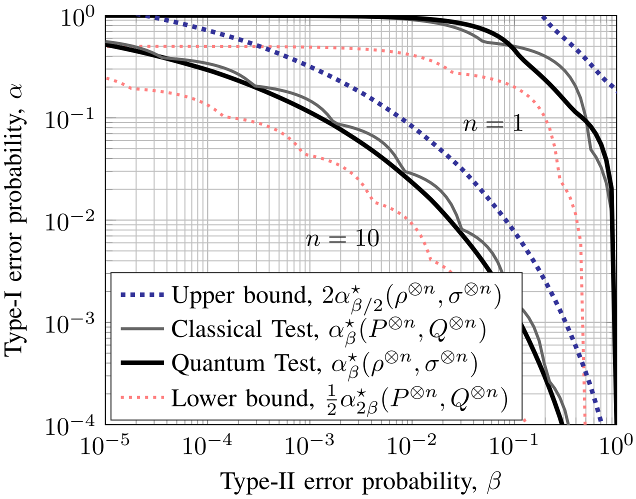

Fig. 3: Error probability trade-off of a hypothesis test between mixed states $\rho^{\otimes n}$ and $\sigma^{\otimes n}$, with ρ and σ given in (41).

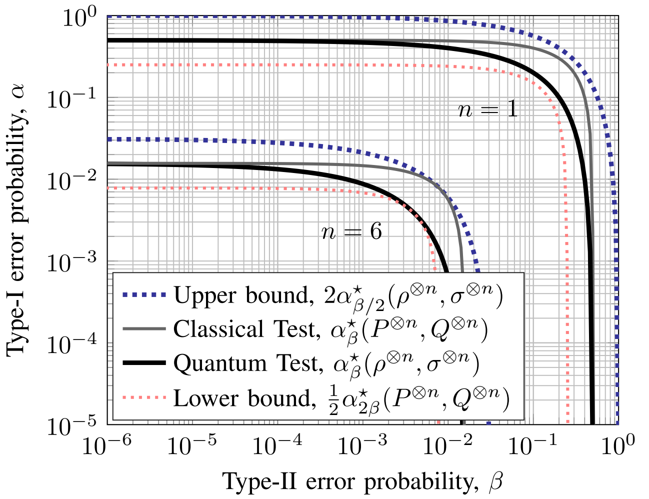

Fig. 4: Error probability trade-off of a hypothesis test between pure states $\rho^{\otimes n}$ and $\sigma^{\otimes n}$, with ρ and σ from (42) when $\phi = \frac{\pi}{4}$.

IV. Numerical Results and Conclusions

We now compare the type-I and type-II error probability trade-off of a quantum hypothesis test with that of the classical hypothesis test resulting from the Nussbaum-Szkoła mapping.

A. Mixed-state discrimination

Consider the quantum states defined by the density operators

$$\rho = \begin{bmatrix} 0.9 & 0 \\ 0 & 0.1 \end{bmatrix}, \qquad \sigma = \begin{bmatrix} 0.5 & 0.4 \\ 0.4 & 0.5 \end{bmatrix}. \tag{41}$$

Both ρ and σ are mixed states with overlapping supports.

Figure 3 compares the error probability trade-off of the quantum hypothesis test $\rho^{\otimes n}$ v. $\sigma^{\otimes n}$ with that of the surrogate classical test $P^{\otimes n}$ v. $Q^{\otimes n}$ defined via the Nussbaum-Szkoła mapping (11)-(12). Even when $n = 1$ both curves exhibit a similar behavior. Note that $P^{\otimes n}$ and $Q^{\otimes n}$ correspond to discrete distributions defined over d^{2n} points, hence their staggered shape when depicted in logarithmic scale (due to the corresponding affine segments in linear scale).

For comparison, we also depict the upper and lower bounds that follow from Theorem 1. Note that in general these bounds are not tight. Moreover, the gap between the upper and lower bound (when plotted in logarithmic scale) is approximately constant with n, as it could be expected due to the multiplicative nature of the bounds that follow from Theorem 1.

B. Pure-state discrimination

We now consider two pure states defined by

$$\rho = \begin{bmatrix} 1 & 0 \\ 0 & 0 \end{bmatrix}, \quad \sigma = \begin{bmatrix} \cos(\phi)^2 & \cos(\phi)\sin(\phi) \\ \sin(\phi)\cos(\phi) & \sin(\phi)^2 \end{bmatrix}. \tag{42}$$

Figure 4 shows the error probability trade-off for the test $\rho^{\otimes n}$ v. $\sigma^{\otimes n}$ with $n = 1$ and $n = 6$, for the states in (42) with $\phi = \frac{\pi}{4}$. For $n = 1$ the inner product between the two states is $a = \mathrm{Tr}[\rho\sigma] = \frac{1}{2}$, and the gap from the error trade-off to the upper and lower bounds is still significant. As the value of n increases, the pure states $\rho^{\otimes n}$ and $\sigma^{\otimes n}$ exhibit a growing degree of orthogonality. In this regime, as shown in Sec. III-B, the lower and upper bound become increasingly tight for the symmetric error probability. This is apparent from Fig. 4, since for $n = 6$ (i.e., $a \approx 0.0156$) the gap between the error curves and the bounds becomes negligible in the region where $\alpha \approx \beta$.

The Nussbaum-Szkoła mapping transforms a hypothesis test between two quantum states into a test between two classical probability distributions. While this mapping was primarily used to study the asymptotics of quantum hypothesis testing as $n \to \infty$, it also approximates its non-asymptotic performance for fixed n. In this work we examine and illustrate the gap between the error probability trade-off of the quantum and classical hypothesis tests in certain settings of interest, laying the groundwork for potential future research in this direction.

References

[1] M. Nussbaum and A. Szkoła, "A lower bound of Chernoff type in quantum hypothesis testing," *arXiv preprint quant-ph/0607216*, 2006.

[2] K. M. R. Audenaert, J. Calsamiglia, R. Munoz-Tapia, E. Bagan, L. Masanes, A. Acin, and F. Verstraete, "Discriminating states: The quantum Chernoff bound," *Physical Review Letters*, vol. 98, no. 16, p. 160501, 2007.

[3] K. M. R. Audenaert, M. Nussbaum, A. Szkoła, and F. Verstraete, "Asymptotic error rates in quantum hypothesis testing," *Communications in Mathematical Physics*, vol. 279, no. 1, pp. 251–283, 04 2008. [Online]. Available: https://doi.org/10.1007/s00220-008-0417-5

[4] F. Hiai and D. Petz, "The proper formula for relative entropy and its asymptotics in quantum probability," *Communications in Mathematical Physics*, vol. 143, no. 1, pp. 99–114, 1991.

[5] T. Ogawa and M. Hayashi, "On error exponents in quantum hypothesis testing," *IEEE Transactions on Information Theory*, vol. 50, no. 6, pp. 1368–1372, 2004.

[6] H. Nagaoka, "The converse part of the theorem for quantum Hoeffding bound," *arXiv preprint quant-ph/0611289*, 2006.

[7] M. Hayashi, "Error exponent in asymmetric quantum hypothesis testing and its application to classical-quantum channel coding," *arXiv preprint quant-ph/0611013*, 2006.

[8] A. B. Coll, G. Vazquez-Vilar, and J. R. Fonollosa, "Generalized perfect codes for symmetric classical-quantum channels," *IEEE Transactions on Information Theory*, vol. 68, no. 9, pp. 5923–5936, Sep. 2022.